Fiber Stipples for Crossing Tracts in Probabilistic Tractography

Submission 1015

Abstract

Given diffusion weighted magnetic resonance (dMRI) data, tractography methods may reconstruct estimations of neural connections of the human brain, so called tractograms. Probabilistic tractography algorithms generate a scalar value for each point of the brain, which describes the confidence of an existing structural connection to a predefined seed region. Recently presented Fiber-Stippling is a promising tool to effectively visualize such scalar values on axis aligned cutting planes. However, Fiber-Stippling only works with principal diffusion directions and cannot handle complex tract configurations, such as overlapping or crossing tracts, which are very important to neuroscience. In this work we present an illustrative technique for probabilistic tracts in such configurations, which is based on Fiber-Stippling. Our technique supports HARDI data and hence can visualize crossing tracts, by keeping all of the advantages of Fiber-Stippling. We solve this by visually supporting the stipples, while not altering the original visualization methaphor. Our work is an important contribution to adequate visualization of neuroanatomy, as crossing tracts are a frequent phenomena inside of the human brain. Moreover, our technique may be customized to crossing line fields in general.

Categories and Subject Descriptors (according to ACM CCS): I.3.3 [Computer Graphics]: Picture/Image Generation—Line and curve generation

1. Introduction

Diffusion weighted resonance imaging (dMRI) is the only imaging modality able to acquire structural connectivity information of the living human brain. Structural connectivity can be roughly understood as the wiring scheme of the brain, where the axonal connections are major building blocks. Neuroscientists aim to analyze certain connections in order to study diseases, development, and structure of the brain.

In practice, there are currently multiple dMRI acquisition schemes which measure the hindrance of water diffusion along different directions. Often, a high number of these so called gradients are used to sample the diffusion profile in each image voxel. The directional measurements are said to be of high angular resolution and, hence, such imaging is called high angular resolution diffusion imaging (HARDI).

Given the measurement data, a diffusion model is fitted to this data. The diffusion tensor, usually depicted as a three-dimensional ellipsoid, is a rather simple, but very popular and wide-spread diffusion model. With the advent

of HARDI more complex diffusion models have been introduced, such as spherical deconvolution [TCC07] and QBall-Imaging [Tuc04]. One of the key advantages of HARDI-based diffusion models over DTI is: HARDI-based diffusion models model more than one diffusion direction per voxel, which is the key for discerning multiple interleaved fiber populations.

One method for identifying structural connections is tractography, which aims at reconstructing neural tracts by tracing paths in dMRI data. However, as the whole pipeline works within millimeter resolution, single axons are far from being captured. Additionally, dMRI data is often highly affected by low signal to noise ratio (SNR), which may cause misleading tracts. Moreover, tracts are known to be arranged in complex configurations, e.g. crossing, bending, kissing, or diverging tracts. Although DTI-based tractography is able to roughly reconstruct plausible anatomical structures, it cannot correctly deal with such configurations. Last but not least, for diffusion tractography there is no ground truth available, and validation is still an open ques-

tion [HP14]. In order to get more confidence in the reconstructed tracts, probabilistic tractography has been proven useful [BSJ14, BBJ∗07].

In this work we present an interactive and illustrative visualization technique, extending Fiber-Stippling [GWG∗11] to support streamline-based probabilistic tracts specifically generated from HARDI data. We maintain the original visualization metaphor wherever possible, but also provide visual support in regions of complex tract configurations. With this work it is now possible to visualize probabilistic tracts even in complex tract configurations, while showing appropriate diffusion directions, connectivity score and anatomical context all at once.

2. Related Work

The related work is structured in three parts: probabilistic tractography methods, visualization of probabilistic tracts, and visualization of crossing line fields.

Probabilistic Tractography: Most of the probabilistic tractography methods employ an altered streamline integration principle, where in each integration step the new direction is randomized regarding the underlying diffusion data. The line-count per voxel is called connectivity score or confidence score (CS) and expresses the confidence that a certain voxel is connected to the seed region. The first streamline-based probabilistic algorithms were presented by Behrens et al. [BWJ∗03] and Parker et al. [PHWK03]. Behrens et al. employed a Bayesian framework for modelling the uncertainty via the probability distribution function (PDF), while Parker et al. used the anisotropy and secondary eigenvectors of the tensors to model the PDF. The bayesian framework approach has been extended to resolve multiple fiber compartments in single voxels cf. [HWA05, BBJ∗07]. Another popular method beside the Bayesian approach is bootstrapping given by Jones et al. [Jon03], which estimates the uncertainty in the orientation distribution function (ODF) by sampling multiple acquisitions and is thus model-free. This approach was further developed by Jones et al. [Jon06] (wild bootstrapping) and by Berman et al. [BCM∗08] (residual bootstrapping), to reduce the required number of image acquisitions. A version of the latter algorithm that used spherical deconvolution instead of QBall imaging was developed by Jeurissen et al. [JLJ∗11]. Aganj et al. [ALJ∗11] introduced a global probabilistic tractography algorithm based on the Hough transform, which also operates on lines as primitives. Our work focuses on the visualization of streamline-based probabilic tractography results from HARDI data, as we use the probabilistic streamlines, also called _proba-fibers_ (cf. Descoteaux et al. [DD08]) for direction estimation of the given tract.

Visualization of Probabilistic Tractography: Recent surveys of visualization techniques for probabilistic tractography are given in [BSJ14, MBWG13, GWG∗11] in-
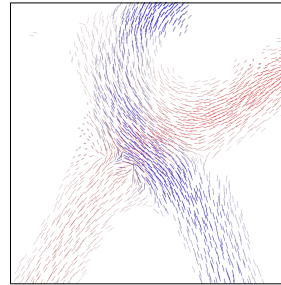

Figure 1: _Two crossing tracts: cortico spinal tract (CST) blue, corpus callosum (CC) red, with the original Fiber-Stippling method [GWG∗11]. As only the principal diffusion direction is available for both tracts, the crossing region is visualized inaccurately._

cluding glyphs, tract density imaging, colormaps, surfaces, volume rendering, and vector plots. Additionally Goldau et al. [GWG∗11] introduced an illustrative visualization technique, called Fiber-Stippling. One of the major advantages over existing techniques is its ability to visualize the connectivity score, principal diffusion orientation and anatomical context, all together on one slice [PHG∗13, MBWG13]. However, Fiber-Stippling is restricted to DTI data and hence cannot adequately visualize HARDI based tractograms nor crossing tracts, as depicted in Fig. 1.

Crossing Line Fields: Crossing structures in the human brain have been visualized in many different ways. Typical examples are rendering diffusion profiles via various types of glyphs, such as multiple vector glyphs per voxel indicating maxima directions (e.g. [BBJ∗07]), or glyphs showing the full ODF or fiber ODF profile [Tuc04, SK10], which are usually normalized to improve perception of the peaks and colored using the typical XYZ to RGB orientation mapping. Another method is rendering the respective tracts using lines. However, this usually results in cluttered images with a high amount of occlusions. A different approach to visualizing crossing structures was presented by Eichelbaum et al. [EHHS12]. They render a fabric-like crossing pattern aligned with the principal and secondary diffusion directions on an arbitrary surface, including slices. While these approaches could be employed for visualizing probabilistic connectivity, they only convey orientation information, but not the confidence score. Another drawback is that usually all orientation information is shown, not just the orientations relevant to some tract of interest.

3. Method

We extend the Fiber-Stippling algorithm of Goldau et al. to be suitable for the visualization of streamline-based probabilistic tractograms generated from HARDI data. The main problem is that HARDI data contains multiple diffusion orientations per voxel and we need to choose the one which matches the local orientation of the tract in order to align the stipples appropriately. We call this **inferring orientations** and present our solution in section 3.1. Furthermore, we propose changes to the original visualization aiming at reducing visual clutter caused by the increased number of visual
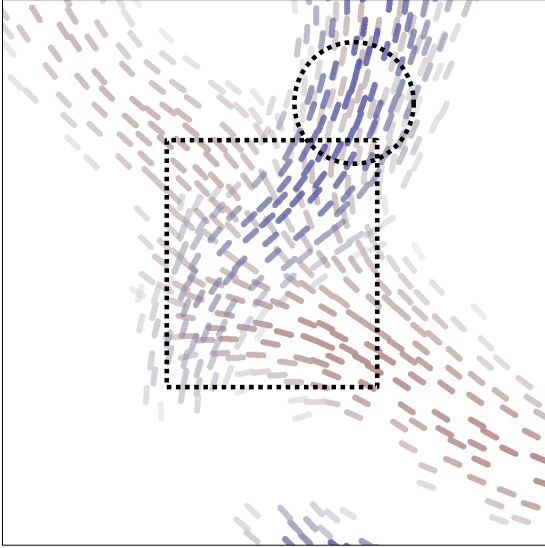
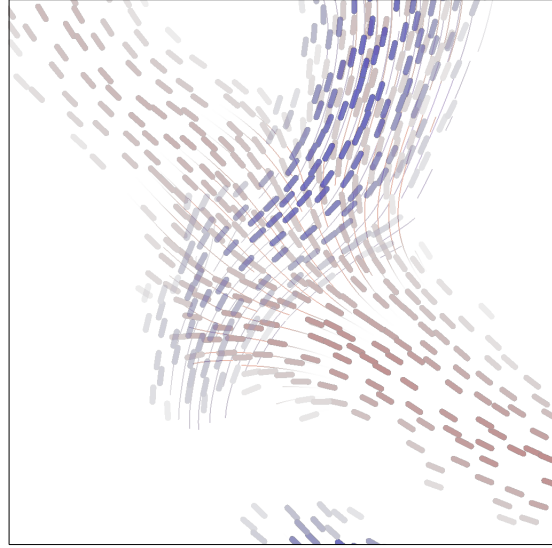**Figure 2:** *Two tracts crossing (box) and merging (circle).*

Figure 3: *Rendering lines as a visual cue to help following tracts.*

primitives: We support **interaction** for focussing on a single tract of interest, and we add **visual cues** to help with visually following tracts through complex configurations, which is important for interactive tract analysis. These methods are discussed in section 3.2.

3.1. Inferring Directions from Tractography Results

We need to choose an appropriate direction from the underlying local diffusion model. In many voxels, this local model contains multiple fiber orientations. Inferring these orientations (i.e. selecting maxima) from the diffusion model is discussed in e.g. [BCM*08, SK10]. and will not be discussed here. The remaining challenge is thus: how to infer the local direction of the tract in order to be able to find the matching local orientation in the model?

As streamline-based probabilistic algorithms operate by generating a large number of tracks starting from a single seed point, we can make use of these proba-fibers, because they explicitly contain the orientation information we require. However, due to the nature of the probabilistic sampling employed in such algorithms, orientations of fibers at some local region in the dataset will naturally form some sort of probability distribution defined on the sphere. Thus, we can calculate a vector field describing the orientation of the tract at each position in the dataset by averaging tangent orientations: Let $\alpha > 0$ be a distance, $\vec{p}$ some position, and $S^{\alpha}(\vec{p})$ the set of track segments for which $\|\vec{p} - \vec{m}_s\| < \alpha$, where $\vec{m}_s$ denotes the midpoint of a segment s. We calculate our average orientation $\vec{v}(\vec{p})$ as a weighted sum over the segment directions in the regions $S^{\alpha}(\vec{p})$:

$$\vec{v} = \text{normalize}\left(\sum_{s \in S^{\alpha}(\vec{p})} \mathcal{N}(|\vec{p} - \vec{m}_s|, \sigma)(\vec{s}_{\text{end}} - \vec{s}_{\text{start}})\right),$$

$$(1)$$

where $\mathcal{N}(\mu, \sigma)$ denotes the normal distribution.

However, this approach alone does not yet produce satisfying results. This is caused by the tracks having similar orientations, but arbitrarily flipped directions. In order to perform correct interpolation of the resulting vectors when rendering the stipples, the vectors need to be aligned to the same directions. To solve this, we employ a preprocessing step which aligns all fibers to the same directions, similar to the preprocessing done by [Gol14]. However, since our tracks are probabilistic and thus much more spurious, we need to use a more robust measure than just the distance between endpoints. Instead, we use the distance function proposed by Garyfallidis et al. [GBC*12, Eqn. 1]:

$$d_{\text{direct}}(s, t) = \frac{1}{K} \sum_{i=1}^{K} |\vec{s}_i - \vec{t}_i|, \qquad (2)$$

$$d_{\text{flipped}}(s, t) = d_{\text{direct}}(s, \text{flip}(t)), \qquad (3)$$

where $\vec{s}_i$ and $\vec{t}_i$ are the ith points of fibers s and t, respectively, and flip(t) simply reverses the order of points in t. This requires all fibers to have the same number of points K, but both doing an equidistant resampling and calculating the distances can be done in linear time, and more importantly, all this can be done in a preprocessing step. Finally, we calculate the mean direction vector field by creating a grid of

a given voxel size which encloses the bounding box of the tracks and then calculating $\vec{v}$ for every grid voxel. If there are no segments in the area induced by α around the voxel position, $\vec{0}$ is used instead. Once the tract direction map is generated, we can use it to identify the best matching maximum in the diffusion model of each voxel. We call the resulting vector field *maxima direction map* and use it as input to the Fiber-Stippling algorithm.

3.2. Interaction and visual cues

When designing the extension to the algorithm, we wanted to keep the original visual metaphor intact. The original Fiber-Stippling algorithm showed various properties of each tract:

- the underlying (local) **orientation** of the tracts by aligning the stipples accordingly in the slice,
- the **angle** the tract has with the slice by adjusting shape of the stipples between long line-like stipples and circles,
- the **confidence** value by a adjusting alpha, color, and density of stipples.

While the first two points are solved by generating an appropriate direction map and then rendering the stipples as usual, we observed the higher number of stipples rendered in crossing regions lead to two distinct problems, as can be seen in Figure 2:

- the confidence values are harder to read
- it gets harder to visually follow the tracts

A useful approach to reducing clutter is to employ the *detail on demand* scheme [Shn96]: If a detailed view on a tract is required by the user, he can select the tract by clicking any stipple in the image. We then change the rendering style of the other tracts to one better suited for displaying context. The latter requires the rendering style to not be distracting. This can be achieved by changing the color to have a much lower saturation. Furthermore, the area of the out-of-focus stipples needs to be reduced in order to minimize the screen space occupied by context information. As the original algorithm explicitly forces all stipples to occupy the same area, this can be achieved by simply changing the area value for out-of-focus tracts; In our implementation, we simply multiply the area by 0.2. By rendering like this, background tracts will show only very thin lines that are much less prominent than the focus tract, yet both the presence and directions of the background tracts can be perceived. As an implementation detail, we also take care of correctly ordering the tracts such that the context is moved to the background and gets occluded by the selected tract. In order to make the selection of focus tracts as easy and natural as possible, we allow the user to click any stipple in the image to select the appropriate tract. Clicking an empty regions deselects the focus and causes all tracts to be rendered normally.

Solving the second issue requires improving the perception of the direction of a path. We thus add another visual cue in the form of lines, which are seeded on the slice using Poisson-Disk sampling similar to the stipples: New lines are started at random locations, follow the orientation field projected into the current slice, and are aborted whenever they get too close to any point on any previous line. The latter is realized via a distance threshold δ_{lines} that is similar to the distance threshold of the stipples. Furthermore, in order to avoid rendering lines in locations where the tract's orientation is perpendicular to the slice, we abort lines if the projected orientation is too small. As they are supposed to only provide visual cues, the lines are rendered in an unobtrusive style by using the tract colors at very low saturation but high brightness (20% and 80%, respectively). This creates the visual impression of lanes on a highway which the stipples follow. Also, we change line alpha depending on the angle between direction field and the slice in order to avoid the lines diminishing the perception of angle. Furthermore, lines are normally restricted to crossing regions only. An example of the resulting visualization can be seen in Figure 3.

4. Data and Preprocessing

We demonstrate the algorithm's ability to convey the properties of probabilistic tractograms in crossing regions using a set of synthetic and human brain data. Pairs of vector fields describing the main diffusion direction and scalar fields mimicking a connectivity map were generated algorithmically for each tract. We generated crossing configurations each containing two three-dimensional, tube-like tracts which cross in angles of 90 degrees, 45 degrees and 26 degrees, respectively. Another configuration contains a section of two crossing circular tracts. Furthermore, we employ the *FiberCup* phantom, which was developed for assessing quality of tractography algorithms and contains many different kissing and crossing configurations [FDG*11]. Finally, test out algorithm on a human brain dwMRI (HARDI) scan acquired on a 3T Siemens Trio MRI scanner using a single echo spin echo EPI sequence with GRAPPA on a 32 channel coil. The image matrix was $128 \times 128 \times 72$ at $1.7 \times 1.7 \times 1.7 \, \text{mm}^3$ voxel size. The data includes 60 gradient ($b = 1000$) and six non-gradient images. The dataset was corrected for motion artifacts using *FSL FLIRT* [JBBS02]. Additionally, the data includes a T1 structural image, which we linearly registered to an FA map generated from the HARDI data using FSL to serve as context for our visualization. From the HARDI data, we also fitted QBalls using the analytical method of Descoteaux [DAFD07], and fiber ODFs using the constrained spherical deconvolution method by Tournier et al. [TCC07] ($l_{max} = 8$ and $\lambda = 0.001$ for both methods).

For the *FiberCup* dataset, we had probabilistic tractograms available that were tracked using an internal implementation of the bootstrapping algorithm of Berman et al. [BCM*08]. 10000 fiber tracks were generated per tract. We used an FA threshold of 0.1, a maximum cur-
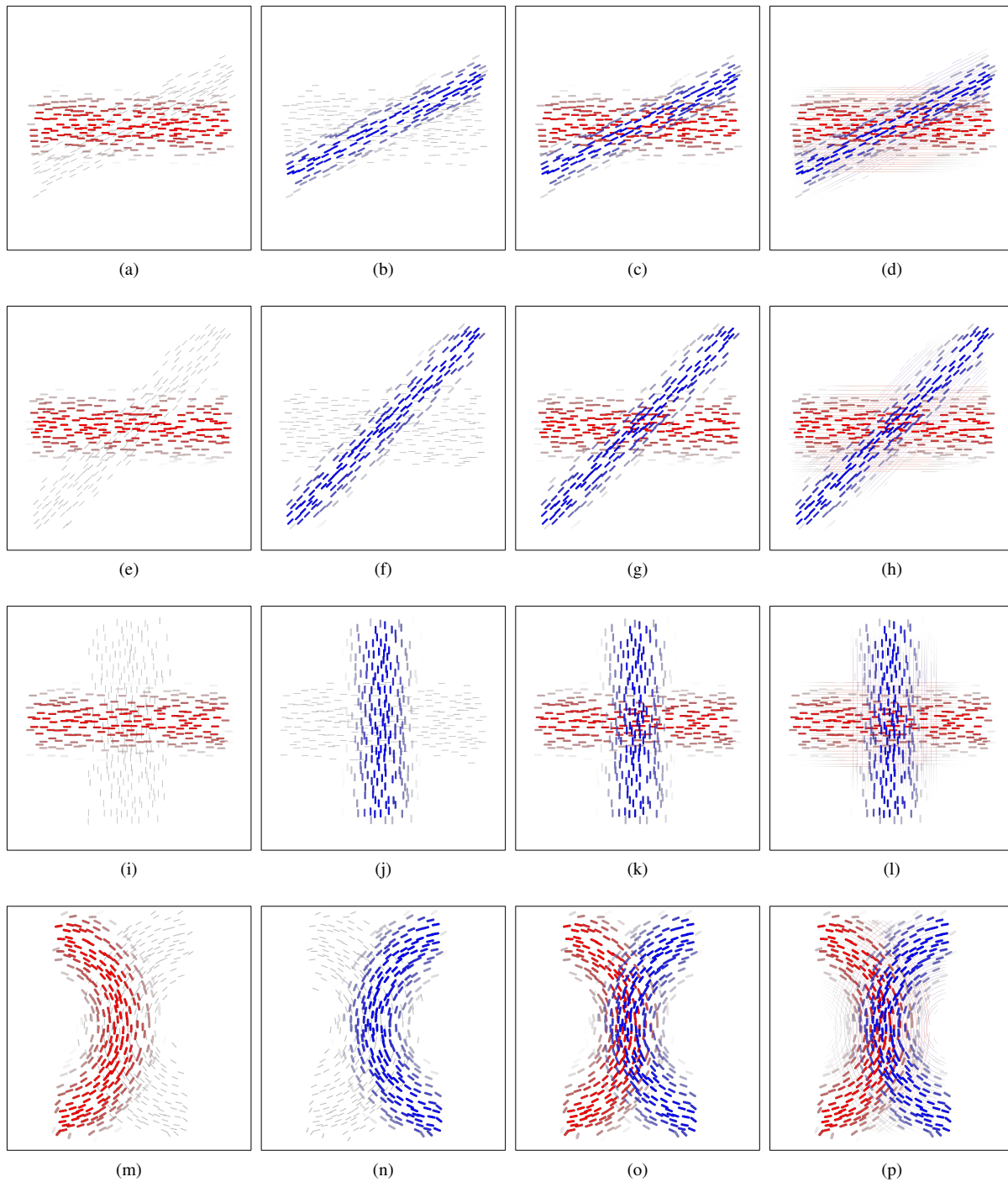
Figure 4: *Synthetic data results. Tracts crossing at (a)-(c) 26 degrees, (d)-(f) 45 degrees, (g)-(i) 90 degrees. (j)-(m): Kissing tracts. Each row shows each of the two respective tracts selected as focus, both tracts selected, and both tracts in combination with line cues.*
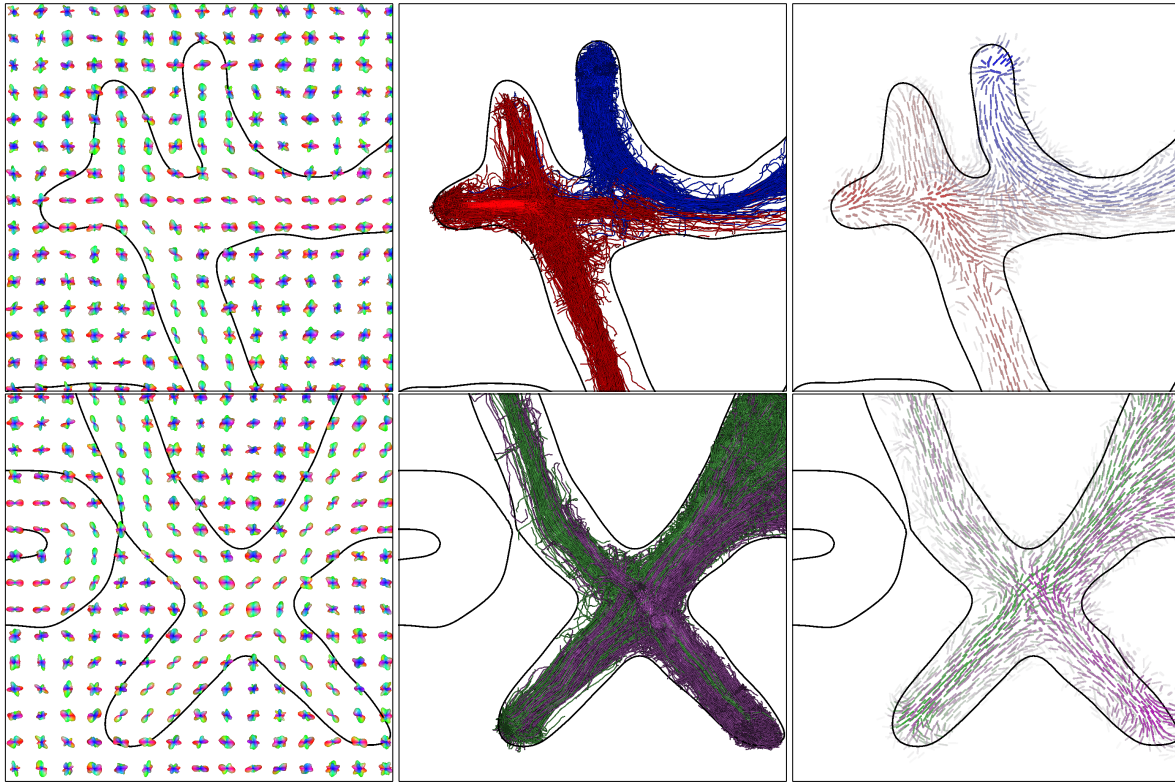
Figure 5: *Showing two tracts per row created on the FiberCup phantom. Left column: QBall glyphs of order six. Middle column: Fiber tracks generated by the tracking algorithm. Right column: Visualization using Fiber-Stippling.*

vature of 75, step size of 0.5mm, and accepted only QBall maxima exceeding 33% of the value of the maximum direction, which were separated by at least 45 degrees from any larger local or global maximum.

For the human brain dataset, probabilistic tractography based on spherical deconvolution was performed using the *mrtrix* toolkit, version 0.2.11 [TCC*12]. One seed point was chosen located in the left and right cortico spinal tracts, the right superior longitudinal fasciculus, the left Cingulum bundle, an u-shaped tract in the left hemisphere, and the corpus callosum tract, respectively. 20 000 fiber tracks were generated per tract using the *SD_PROB* method and then converted to vkt "LINES" format for loading into our visualization toolkit. We used the standard parameters as suggested on their website. Furthermore, we used the fiber ODFs calculated by spherical deconvolution and each tract's direction map (calculated as described in section 3.1, $\sigma = 2$mm, voxel size 1.7mm) to calculate the maxima direction map used to align the stipples.

5. Results

We demonstrate our visualization on a variety of datasets: Figure 4 shows our stippling for the four synthetic datasets.

For every dataset, we show both tracts and each tract as a focus in separate images, respectively. Only the averaged direction map is shown, diffusion model maxima were not available. The directions of the tracts can easily be seen, and focussing a tract allows for the perception of the confidence values in the crossing areas. Another synthetic dataset is the FiberCup phantom, for which we also created four tractograms. Per row, two resulting tracts are shown in Figure 5. For comparison, the fibers and QBalls are also shown. The images using Fiber-Stippling allow us to get an overview over both the orientations and confidence values at the same time.

For the human brain data, we show the six generated tracts all at the same time in figure 6. A closeup of the crossing region (A) demonstrates the advantages of the technique: The three tracts can easily be told apart by their color. The crossing is clearly visible and the stipples are aligned as we would expect, even in the part of the CC tract that diverges into the superior part of the CST tract. When comparing the stipple orientation between using the fiber direction maps and the maxima direction maps, we found that changes in the orientations are only visible in very few places that are mostly located at the edges of the tracts, in regions exhibiting low
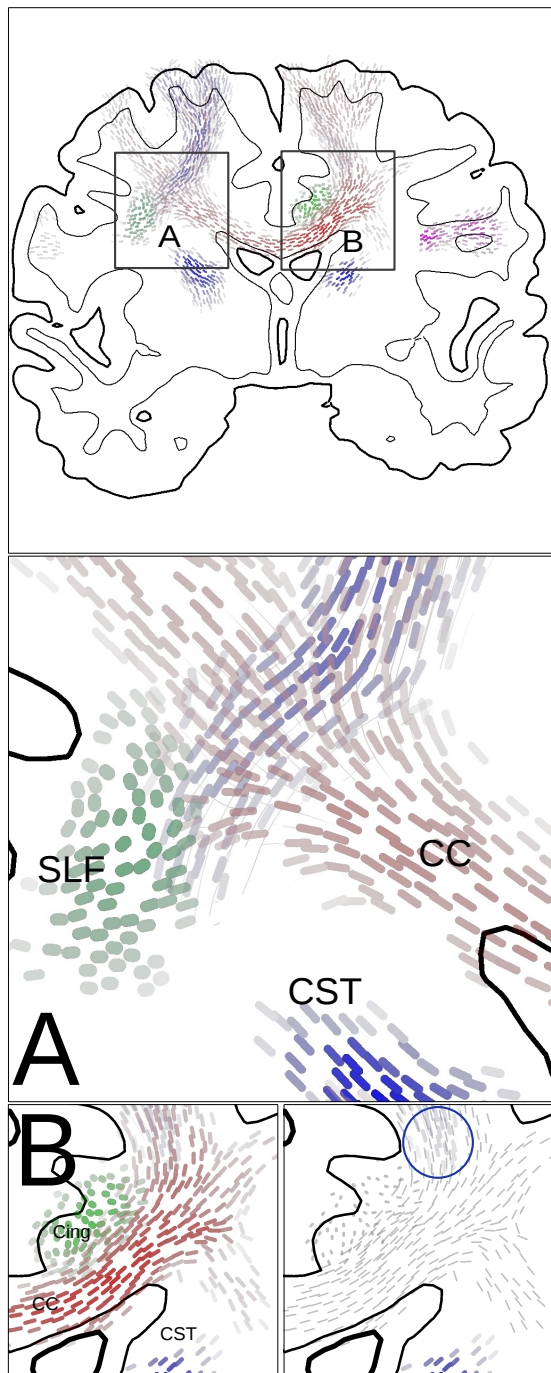
confidence values. Concerning interactivity, the visualization runs at interactive frame rates (average 34.2 frames per second) on a workstation equipped with a dual Intel Xeon E5-2630v3 CPU, 32GB RAM, and an NVIDIA GeForce GTX 980 graphics card, even when showing all six tracts at once at a stipple resolution of 0.002 as in the images.

Finally, figure 7 shows different versions of the orientation cues in action: An image without cues (7a) is compared to cues everywhere along the tracts (7b), cues only in the crossing region (7c), and cues shaded according to the angle of the tract orientation and the slice normal. The lines help with the perception of the exact path each tract takes in the crossing region. However, we found that the lines need to be seeded sparsely in order to not cause visual clutter.

6. Discussion

In this paper, we presented an extension of the Fiber-Stippling algorithm of Goldau et al. [GWG*11], which eliminates its weakness of not being able to correctly display crossing (or otherwise overlapping) probabilistic tractograms.

By changing the input field from principal diffusion orientations computed from DTI to an appropriately constructed direction field, we allow the algorithm to show tract-specific stipple orientations in crossing regions. The resulting stipples align well with the directions the tracts propagate into, which we have shown in our resulting images. In those images, it is easy to identify where crossings of tracts happen and to roughly determine the direction of each tract involved. By reducing the density of the stipples, the image becomes clearer, but at the cost of being able to read the tract's confidence value. It is also possible to see the tracts diverging. This property also allows us to compare tracts which were seeded from similar locations, and are thus likely the exhibit similar spatial confidence maps.

This has the advantage of not requiring the underlying diffusion model used by the tracking algorithm in order to show meaningful images. As we only need to interpolate in a 3D vector field to determine the stipple orientations (which can easily be done in shaders), we can achieve interactive frame rates.

We also provided a method for precomputing the required direction field from the proba-fibers generated by the tractography algorithms. Using either the fiber direction map or the maxima direction map allows us to compute stipple orientations very quickly by means of simple interpolation, which can be done by the graphics hardware. A more accurate way to compute maxima directions would be to interpolate the HARDI data at every stipple position and then extract the maxima, but this would require recomputation whenever the slice position changes. As this would be a very expensive operation (a prototype implementation had an update time in the order of seconds per tract), and the stipple

Figure 6: *Resulting visualization for six probabilistic tractograms using the maxima direction map to compute stipple orientation. (A) Region of crossing tracts: cortico-spinal tract (CST, blue), corpus callosum (CC, red), superior longitudinal fasciculus (SLF, green). (B) Using interaction to focus the right-hand side cortico-spinal tract reveals a low-confidence area marked by the blue circle. All images are shown from an anterior view.*
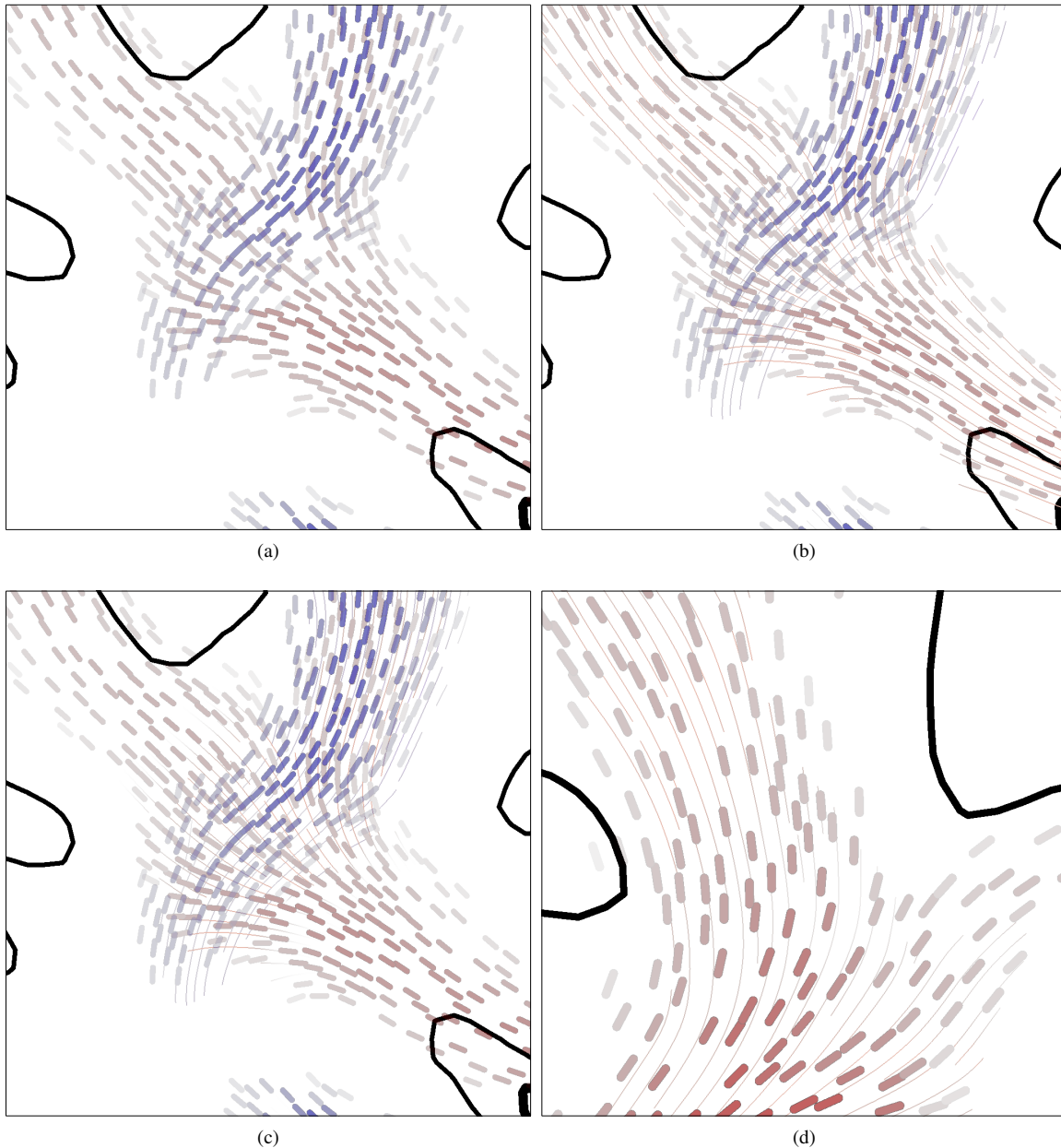
Figure 7: *Visual cues for the orientations of the tracts. (a) Without cues. (b) Showing cues everywhere. (c) Only regions shared by multiple tracts. (d) Additional transparency based on the angle to the slice; shown in a different area.*

orientation computed only changes slightly in mostly low confidence locations, we favor using the maxima direction field computed from the proba-fibers and the local model. Furthermore, our experiments indicated that it even suffices to directly use the fiber direction map. This has the advantage of only relying on the output of the tracking algorithm, as no local model is required. This is possible because the

proba-fibers already contain the necessary information about the orientation field. However, for this to work, the number of tracks to average is important, and thus the errors are largest in regions of low track density, i.e. regions of low confidence. For this reason, choosing the right values for α and σ is crucial, because of too much smoothing or too few segments averaged for too large and small values, respec-

tively. Setting $\sigma = 2$mm and $\alpha = 2\sigma$ worked well in our experience.

A disadvantage of our method is that not all probabilistic tractography algorithms produce tracks, which limits our approach to only a subset of all available algorithms. While most of the probabilistic algorithms to date produce a set of lines at least internally, so changing the algorithms to output these lines should be trivial, future algorithms might use different tracking strategies.

Besides the computation of the stipple orientations, the other two important extensions we proposed were the use of *detail on demand* by allowing to choose tracts of interest and the addition of visual cues to aid in visually tracking tracts even through densely sampled regions. By selecting a tract of interest and hiding the confidence values of the other tract, the perception of the confidence values of the selected tract becomes easily possible, while still providing enough hints on the presence and orientation of other tracts, thus preserving the mental map through the change in presentation. Doing selection via clicking the tract of interest directly in the image (as opposed to e.g. using some UI widget) is a most intuitive way of handling the interaction. Concerning the second extension, the use of lines as primitives has two decisive advantages: They do not occupy much screen space and thus preserve context; and the human eye is able to track lines through discontinuities (caused by being occluded by stipples) – as long as they do not get too large – unconsciously, i.e. without the user having to concentrate on them. Also note how the lines in the images follow the orientation of the tracts, forming a visual impression of a highway. We managed to extend the Fiber-Stippling method without destroying the original visualization metaphor.

We should note that fiber stipples are actually a glyph-based visualization technique, so for future work, it seems natural to evaluate whether changing the stipples to convey additional properties (similar to e.g. [Jon03]) via shape may be possible without visually overloading the images.

7. Conclusion

We have presented an extension of the Fiber-Stippling algorithm that is, to our knowledge, the first visualization able to comprehensively present crossing probabilistic tracts. The method's advantage over other approaches is its ability to communicate context, confidence score, and direction/orientation of multiple tracts at once in a single image. We extract the required per-tract orientation map in a pre-processing step, leaving the visualization itself interactive. Using *detail on demand* allows us to view tract parameters without distracting context. We also support visual tracing of bundles in crossing and even diverging configurations by introducing highway-like visual cues in the form of lines.

References

[ALJ*11] AGANJ I., LENGLET C., JAHANSHAD N., YACOUB E., HAREL N., THOMPSON P. M., SAPIRO G.: A hough transform global probabilistic approach to multiple-subject diffusion mri tractography. *Med. Image Anal. 15*, 4 (2011), 414–425. 2

[BBJ*07] BEHRENS T., BERG H. J., JBABDI S., RUSHWORTH M., WOOLRICH M.: Probabilistic diffusion tractography with multiple fibre orientations: What can we gain? *Neuroimage 34*, 1 (2007), 144–155. 2

[BCM*08] BERMAN J. I., CHUNG S., MUKHERJEE P., HESS C. P., HAN E. T., HENRY R. G.: Probabilistic streamline q-ball tractography using the residual bootstrap. *Neuroimage 39*, 1 (2008), 215–222. 2, 3, 4

[BSJ14] BEHRENS T. E., SOTIROPOULOS S. N., JBABDI S.: Chapter 19 - MR diffusion tractography. In *Diffusion MRI (2nd Ed.)*, Johansen-Berg H., Behrens T. E., (Eds.), second edition ed. Academic Press, San Diego, 2014, pp. 429–451. 2

[BWJ*03] BEHRENS T., WOOLRICH M., JENKINSON M., JOHANSEN-BERG H., NUNES R., CLARE S., MATTHEWS P., BRADY J., SMITH S.: Characterization and propagation of uncertainty in diffusion-weighted mr imaging. *Magn. Reson. Med. 50*, 5 (2003), 1077–1088. 2

[DAFD07] DESCOTEAUX M., ANGELINO E., FITZGIBBONS S., DERICHE R.: Regularized, fast, and robust analytical q-ball imaging. *Magn. Reson. Med. 58*, 3 (2007), 497–510. 4

[DD08] DESCOTEAUX M., DERICHE R.: Mapping neuronal fiber crossings in the human brain. *SPIE Newsroom (August 2008)* (2008). 2

[EHHS12] EICHELBAUM S., HLAWITSCHKA M., HAMANN B., SCHEUERMANN G.: Image-space tensor field visualization using a lic-like method. In *Visualization in Medicine and Life Sciences II*. Springer, 2012, pp. 191–208. 2

[FDG*11] FILLARD P., DESCOTEAUX M., GOH A., GOUTTARD S., JEURISSEN B., MALCOLM J., RAMIREZ-MANZANARES A., REISERT M., SAKAIE K., TENSAOUTI F., ET AL.: Quantitative evaluation of 10 tractography algorithms on a realistic diffusion mr phantom. *Neuroimage 56*, 1 (2011), 220–234. 4

[GBC*12] GARYFALLIDIS E., BRETT M., CORREIA M. M., WILLIAMS G. B., NIMMO-SMITH I.: Quickbundles, a method for tractography simplification. *Frontiers in neuroscience 6* (2012). 3

[Gol14] GOLDAU M.: *Multi-Modal and Slice-Based Visualizations of Diffusion Tractography Data*. PhD thesis, Leipzig University, 2014. 3

[GWG*11] GOLDAU M., WIEBEL A., GORBACH N. S., MELZER C., HLAWITSCHKA M., SCHEUERMANN G., TITTGEMEYER M.: Fiber stippling: An illustrative rendering for probabilistic diffusion tractography. In *Biological Data Visualization (BioVis), 2011 IEEE Symposium on* (2011), IEEE, pp. 23–30. 2, 7

[HP14] HUBBARD P. L., PARKER G. J.: Chapter 20 - validation of tractography. In *Diffusion MRI (2nd Ed.)*, Johansen-Berg H., Behrens T. E., (Eds.), second edition ed. Academic Press, 2014, pp. 453–480. 2

[HWA05] HOSEY T., WILLIAMS G., ANSORGE R.: Inference of multiple fiber orientations in high angular resolution diffusion imaging. *Magn. Reson. Med. 54*, 6 (2005), 1480–1489. 2

[JBBS02] JENKINSON M., BANNISTER P., BRADY M., SMITH S.: Improved optimization for the robust and accurate linear registration and motion correction of brain images. *Neuroimage 17*, 2 (2002), 825–841. 4

[JLJ*11] JEURISSEN B., LEEMANS A., JONES D. K., TOURNIER J.-D., SIJBERS J.: Probabilistic fiber tracking using the residual bootstrap with constrained spherical deconvolution. *Hum. Brain Mapp. 32*, 3 (2011), 461–479. 2

[Jon03] JONES D. K.: Determining and visualizing uncertainty in estimates of fiber orientation from diffusion tensor mri. *Magn. Reson. Med. 49*, 1 (2003), 7–12. 2, 9

[Jon06] JONES D.: Tractography gone wild: Probabilistic tracking using the wild bootstrap. In *Proc ISMRM* (2006), p. 435. 2

[MBWG13] MARGULIES D. S., BÖTTGER J., WATANABE A., GORGOLEWSKI K. J.: Visualizing the human connectome. *Neuroimage 80* (2013), 445–461. 2

[PHG*13] PELZER E. A., HINTZEN A., GOLDAU M., VON CRAMON D. Y., TIMMERMANN L., TITTGEMEYER M.: Cerebellar networks with basal ganglia: feasibility for tracking cerebello-pallidal and subthalamo-cerebellar projections in the human brain. *Eur. J. Neurosci.* (2013), 3106–3114. 2

[PHWK03] PARKER G. J., HAROON H. A., WHEELER-KINGSHOTT C. A.: A framework for a streamline-based probabilistic index of connectivity (PICo) using a structural interpretation of mri diffusion measurements. *J. Magn. Reson. Imaging 18*, 2 (2003), 242–254. 2

[Shn96] SHNEIDERMAN B.: The eyes have it: A task by data type taxonomy for information visualizations. In *Visual Languages, 1996. Proceedings., IEEE Symposium on* (1996), IEEE, pp. 336–343. 4

[SK10] SCHULTZ T., KINDLMANN G.: A maximum enhancing higher-order tensor glyph. In *Computer Graphics Forum* (2010), vol. 29, Wiley Online Library, pp. 1143–1152. 2, 3

[TCC07] TOURNIER J.-D., CALAMANTE F., CONNELLY A.: Robust determination of the fibre orientation distribution in diffusion mri: non-negativity constrained super-resolved spherical deconvolution. *Neuroimage 35*, 4 (2007), 1459–1472. 1, 4

[TCC*12] TOURNIER J., CALAMANTE F., CONNELLY A., ET AL.: Mrtrix: diffusion tractography in crossing fiber regions. *International Journal of Imaging Systems and Technology 22*, 1 (2012), 53–66. 6

[Tuc04] TUCH D. S.: Q-ball imaging. *Magn. Reson. Med. 52*, 6 (2004), 1358–1372. 1, 2